CORROSION PRODUCT CHARACTERISATION BY FIBRE OPTIC RAMAN SPECTROSCOPY

D.A. Guzonas, P.A. Rochefort and C.W. Turner

ABSTRACT

Fibre optic Raman spectroscopy has been used to characterise secondary-side deposits removed from CANDU® steam generators. The deposits examined were in the form of powders, millimetre-sized flakes, and deposits on the surfaces of pulled steam generator tubes. The compositions of the deposits obtained using Raman spectroscopy are similar to the compositions obtained using other ex-situ analytical techniques. A semi-quantitative estimate of amounts of the major components can be obtained from the spectra. It was noted that the signal-to-noise ratio of the Raman spectra decreased as the amount of magnetite in the deposit increased, as a result of absorption of the laser light by the magnetite. The conversion of magnetite to hematite by the laser beam was observed when high laser powers were used. The Raman spectra of larger flake samples clearly illustrate the inhomogeneous nature of the deposits.

Atomic Energy of Canada Limited
Chalk River Laboratories
Chalk River, Ontario, Canada K0J 1J0

INTRODUCTION

Fouling of the secondary-side of nuclear steam generators (SGs) by corrosion products and other impurities that have been transported into the boiler with the feedwater is a serious problem. Deposit build-up on boiler tubes can lower the rate of heat transfer,[1,2] whereas the build-up of deposits within the tube support structure can lead to density wave oscillations[3] in recirculating SGs and flooding of the steam aspirator ports in once-through SGs.[4] Deposits can act as sites for the concentration of impurities leading to localised corrosion of the underlying substrate. When fouling is severe, the deposits must be removed by chemical and/or mechanical cleaning techniques. The deposit composition is then required to optimise the cleaning conditions and procedures. The composition of the deposits also provides information on the chemistry conditions within the SG and the feedtrain itself.[5,6]

Although deposit samples can be removed from the steam generator (for example, after waterlancing) the quantity of deposit available is often limited. The exact origin within the steam generator of the deposit recovered is not always known, and the samples may undergo surface alteration upon exposure to the atmosphere. An *in-situ* inspection technique capable of identifying the chemical compounds present in a deposit, and of giving a semi-quantitative measurement of their concentrations, would therefore provide valuable information. With an appropriate delivery system, difficult-to-access areas, such as crevices, where sample removal for ex-situ characterisation is difficult, could also be examined.

Recent advances in instrumentation make Raman spectroscopy a useful method for the remote characterisation of materials by vibrational spectroscopy. Fibre optics provide a simple and low cost method of obtaining in-situ Raman spectra from remote areas. In the past decade, various approaches to fibre optic Raman spectroscopy have been developed[7]. Remote Raman spectroscopy using fibre-optics now is being used in plant environments to characterise a variety of materials.[8]

In an ongoing program to develop and demonstrate fibre-optic Raman probes for the in-situ characterisation of secondary-side deposits, we have constructed several fibre optic probes capable of measuring Raman spectra of secondary-side deposits. The use of these probes to measure the Raman spectra of oxides found in CANDU secondary side deposits, and to measure the spectra of secondary-side deposits removed from boilers at CANDU nuclear generating stations is described in this paper.

EXPERIMENTAL

Raman spectra were measured using a fibre optic collection system coupled to a SPEX 1000M single monochromator equipped with a SPEX SPECTRUM ONE charge-coupled device (CCD) detection system and SPEX DM3000 software. The detector integration times and the number of acquisitions that were signal-averaged were optimised to give the best signal-to-noise ratio for each sample. Typically, 10- to 40-second integration times and 4 to 16 acquisitions were used. The 647.1 nm line from a krypton ion laser was used for excitation. The laser power incident on the samples was approximately 30 mW.

Raman spectra were acquired over the range 150-1600 cm^{-1} in several overlapping windows, which were then spliced together. Data manipulations such as baseline correction and spectral splicing were carried out using the GRAMS/386 software package (Galactic Industries Inc.).

The optical requirements for measurement of Raman spectra using fibre optics have been thoroughly discussed in the literature.[7] Optical filtering is required to minimise the effect of Raman scattering in the silica fibres used to bring the laser beam to the sample and to collect the scattered light from the sample. A bandpass filter is required for the input laser light to remove the silica Raman scatter from the fibre, and a notch filter is required for the collected light to reject the laser light and allow only the Raman scatter to enter the collection optics.

Figure 1 shows a schematic of the basic optical arrangement we have used in both laboratory and prototype field probes. The design is centred around the use of a holographic notch filter (Kaiser Optical Inc.) as both a reflective optical component for the incident laser light, and as a notch filter for the Raman scattered light. The laboratory optical assembly (Figure 1) is approximately 200 mm long and 40 mm in diameter. The input laser beam enters near the base of the assembly at right angles to the optical axis and reflected by an adjustable mirror onto the center of the notch filter. The position and angle of the mirror is adjusted to reflect the laser beam from the filter and along the optical axis through a 0.4 numerical aperture (NA) long working distance microscope objective (Leitz H32X/0.60). The sample is placed at or near the focal point of the beam, and scattered light from the sample is collected and collimated by the objective and directed back up to the notch filter. Rayleigh scattered light (having the same wavelength as the incident beam) is reflected by the notch filter, whereas Raman-shifted light is transmitted through the filter. The Raman signal is concentrated by a condenser lens onto the end of a fibre optic bundle and transmitted to the spectrometer. The use of a single objective to both focus the laser beam and collect the scattered light significantly reduces the alignment complexity, compared to a two lens optical arrangement (one to focus the laser beam and one to collect the scattered light).

The collection fibre optic bundle consists of seven step-index multimode fibres having 200 μm pure silica cores, terminated at each end with modified SMA fibre optic couplers. At the collection end, the fibres are arranged in a six-around-one close-packed geometry, while at the other end, coupled to the spectrometer, the fibres are arranged in a close-packed line. At both ends the fibres are polished flat. The output of the fibre bundle is focused on the slits of the spectrometer by a pair of camera lenses chosen to match the NA of the fibres to the NA of the spectrometer.

The optical layout of the prototype secondary side probe was similar to that of the laboratory optical probe, with the exception that the laser beam was carried to the probe by a single-mode fibre, and there was no bandpass filter on the input laser beam. The prototype probe was constructed using miniature optics, and the final size was 6.5 cm x 8.0 cm x 2.0 cm. The size could not be significantly reduced further, due to the holographic notch filter manufacturers size limitations (diameter no smaller than 8 mm).

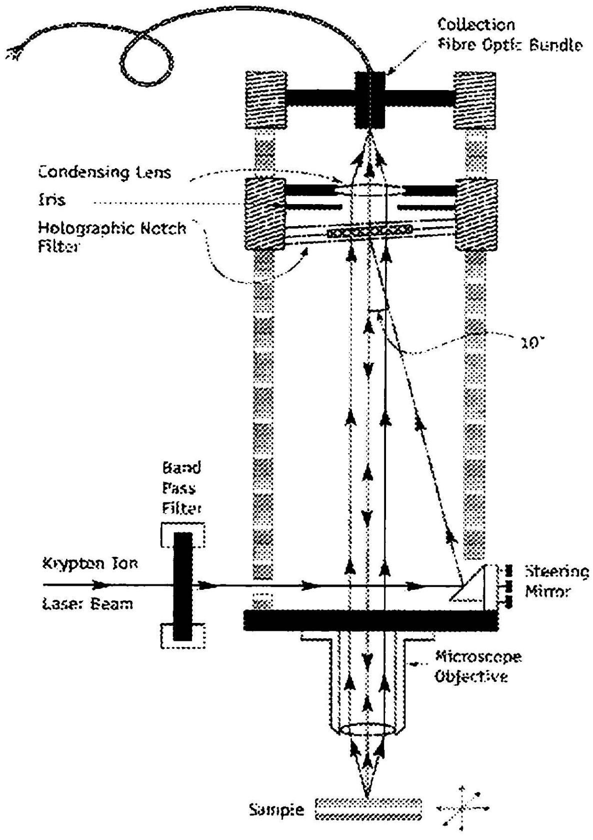

FIGURE 1: Diagram of the Optical Configuration used in the Raman Probes.

The deposit samples examined were from Bruce Nuclear Generating Station (BNGS) Units 2 and 3, Pickering Nuclear Generating Station (PNGS) Units 5 and 6, and Gentilly-2 Nuclear Generating Station (G-2). Most of the samples investigated were deposits that had been removed from steam generators by waterlancing, and were in the form of loose powders, or millimetre-sized flakes of irregular shape. Raman spectra were also obtained from deposits on the secondary side of small (0.5 cm x 0.5 cm) sections of steam generator tubes pulled from steam generators. A detailed analysis of the BNGS Unit 2 and PNGS Unit 5 samples using XRD, energy dispersive X-ray (EDX), X-ray photoelectron spectroscopy (XPS), Mossbauer spectroscopy, inductively coupled plasma atomic emission spectroscopy (ICP-AES), and neutron activation analysis (NAA) had been performed previously. These compositional analyses enabled a comparison of the quantitative results obtained using fibre-optic Raman spectroscopy with those obtained using more common analytical techniques.

About 0.1 g of the powder or flake sample was placed in a Teflon-lined dish and a small amount (<1mL) of water added to simulate the wet conditions expected during an in-situ inspection of deposits in a steam generator. The presence of water was found to reduce laser damage to the samples. The wetted sample was placed at the focus of the collection optics, about 5 mm from the collection lens.

It was much easier to obtain Raman spectra from samples that contained low concentrations of magnetite. The signal-to-noise ratio of the Raman spectra decreased significantly as the amount of magnetite in the deposit increased, as a result of the strong absorption of the laser light by magnetite. Sample degradation, often indicated by the appearance of strong hematite bands in the Raman spectrum after short exposure to the laser beam, occurred unless care was taken to optimise the laser power and focusing. A red-coloured damage zone could often be observed where the laser beam had struck the sample. To obtain spectra with a reasonable signal-to-noise ratio, aquisition times of 2-5 min were required for the samples with low magnetite, while 5-10 min were required for the samples with high magnetite content.

RESULTS AND DISCUSSION

Fibre Optic Raman Spectroscopy of Iron Oxides

The Raman spectra of the iron oxide phases expected in CANDU secondary side deposits have been well documented in the literature.[9-11] Most of the iron oxides studied give reasonably intense and distinct Raman spectra; feroxyhyte and ferrihydrite have only weak, broad bands which would be hard to detect in complex mixtures like secondary side deposits. The spinel phases have similar spectra, but the band frequencies are different enough to enable them to be distinguished in a mixture. To test the fibre optic probe designs, Raman spectra of iron oxide reference samples were measured; the measured band frequencies are tabulated in Table 1. The Raman spectra of the three most common iron oxide phases found in the CANDU deposits (magnetite, hematite and nickel ferrite), measured using the laboratory Raman probe, are shown in Figure 2. A Raman spectrum of magnetite, measured using the prototype field probe, is shown in Figure 3. These spectra demonstrate that the fibre optic probe designs constructed are suitable for the characterisation of the iron oxides found in CANDU deposits.

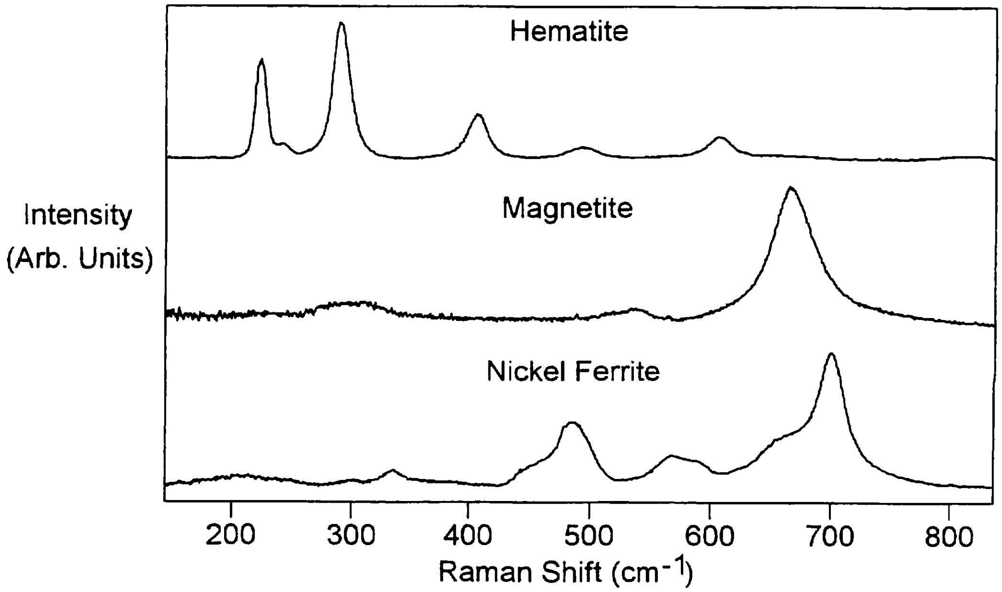

FIGURE 2: Raman Spectra of the Three Principal Iron Oxides found in CANDU Secondary Side Deposits.

TABLE 1: MEASURED RAMAN BAND FREQUENCIES FOR ELEVEN IRON OXIDE PHASES

Oxide		Band Frequency (cm^{-1})								
Spinel Group	Magnetite Fe_3O_4		292 w*	309 w			535 w		666 s	
	Nickel Ferrite $NiFe_2O_4$		292 w	325 w	455 w, br	485 m	570 w		660 m, sh	700 s
	Copper Ferrite $CuFe_2O_4$					485 m, br	553 w	609 w		704 s
	Zinc Ferrite $ZnFe_2O_4$			300 w	344 m	476 w,br			641 s,br	
FeOOH Group	Goethite α-FeOOH		245 m	300 s	387 s	481 m	549 w			
	Akaganeite β-FeOOH		248 w	300 m	386 m	413 w	483 w	542 w		
	Lepidocrocite γ-FeOOH		248 s	347 w	378 m			526 w		
	Feroxyhyte δ-FeOOH								679 w,br	
Fe_2O_3 Group	Hematite α-Fe_2O_3	225 s	243 w	300 s		409 m	495 w	611 m	656 w	
	Maghemite γ-Fe_2O_3		256 w	284 w	334 s,br	376 s,br	500 s,b	625 m,sh	654 s,br	711 s
	Ferrihydrite $Fe_2O_3 \cdot 3H_2O$						507 w,br	615 w		712 w,br

w - weak m - medium s - strong br - broad sh - shoulder.

* may be a hematite band (from laser-induced conversion of magnetite to hematite)

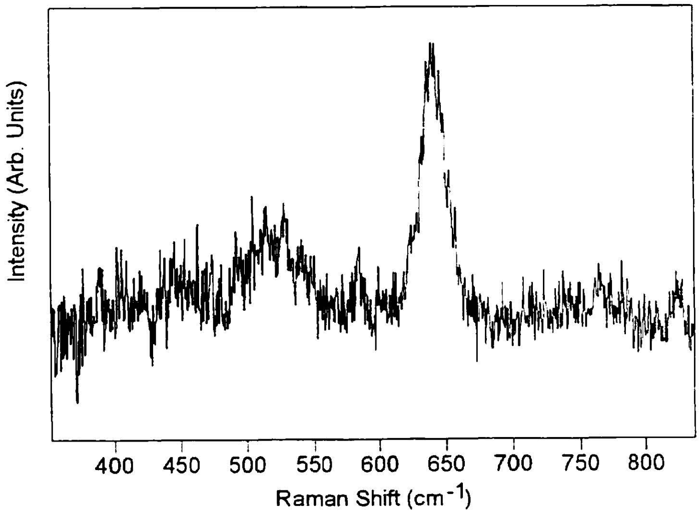

FIGURE 3: Raman Spectrum of Magnetite Obtained with the Prototype Secondary Side Probe

Raman Analysis of Field Samples

Representative Raman spectra of four of the secondary-side deposits, measured using the laboratory probe, are shown in Figure 4. The spectra from the PNGS samples (Unit 5 and Unit 6) contain a strong band envelope in the 640-710 cm^{-1} region characteristic of nickel ferrite. This band overlaps with the strongest magnetite band at approximately 665 cm^{-1}. It is apparent that Raman spectroscopy can readily and unambiguously identify the presence of nickel ferrite in these deposits. The PNGS Unit 5 and Unit 6 spectra are slightly different, suggesting different concentrations of nickel ferrite in the two deposits. The semi-quantitative estimation of these concentrations will be discussed later in the paper.

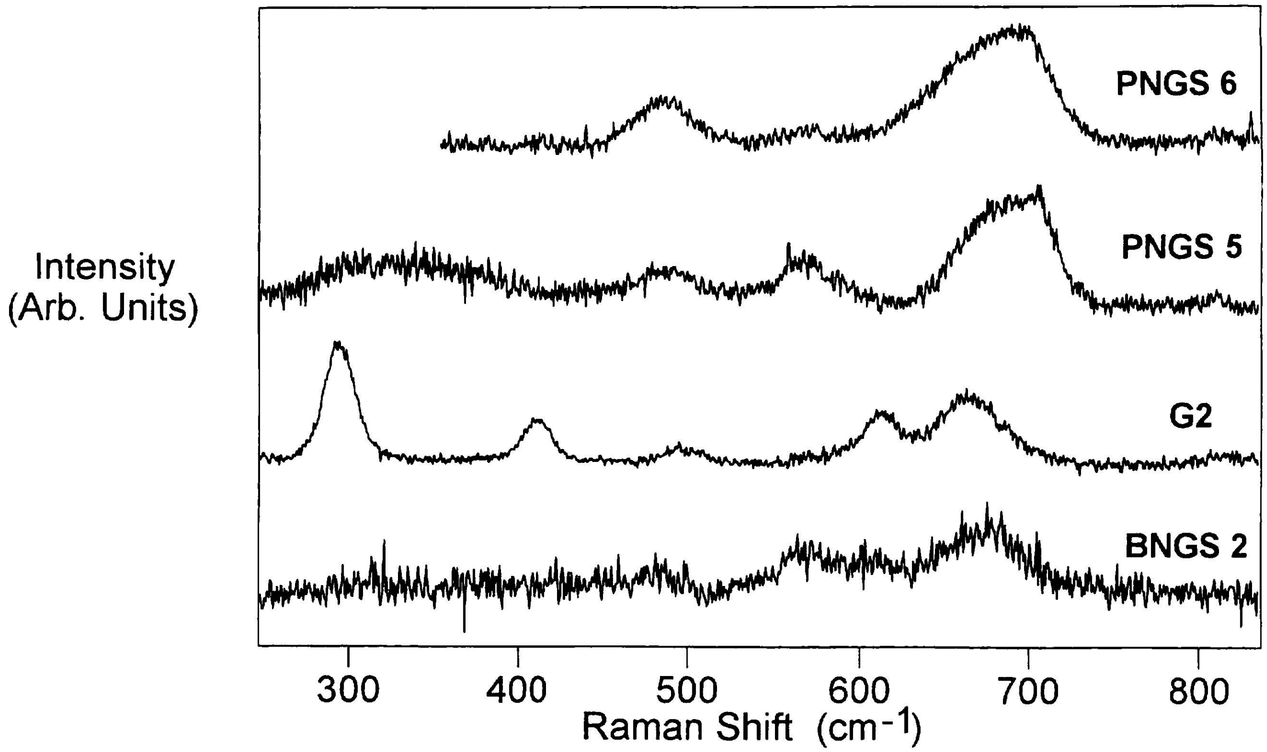

FIGURE 4: Raman Spectra of Secondary Side Deposits from Several CANDU stations.

The Raman spectrum of the Gentilly-2 deposit shows the presence of both hematite and magnetite (cf. Figure 2). In addition, a band of unknown origin was observed at 1088 cm^{-1} (not shown), possibly due to a carbonate species; calcium carbonate has a strong Raman band at about 1085 cm^{-1}.[12]

The loose powder deposits from BNGS Unit 2 were highly sensitive to damage from the focused laser light. The weak Raman scattering from the strongly absorbing black sample required long integration times to achieve a good signal-to-noise ratio. It was more difficult to obtain spectra from these samples than from synthetic deposits prepared with similar amounts of magnetite, suggesting that other impurities in the Bruce deposits contributed to the poor Raman signal. The Raman spectrum of the BNGS Unit 2 powder sample contains bands due to magnetite, and a weak band at 609 cm^{-1} of unknown origin.

The BNGS flake samples from Unit 3 showed interesting variations between flakes and from point to point within the same flake (Figure 5). This variation is not surprising as the exact origin of the flake samples within the steam generator is unknown. Some insight into the significance of these composition differences could be obtained from *in-situ* deposit characterisation. The Raman spectrum obtained from the first flake (Flake 1 in Figure 5) contained only bands arising from magnetite. On the second flake, some regions gave rise to spectra containing only magnetite bands (similar to Flake 1). The spectra from other regions (Flake 2 in Figure 5) contained a strong, broad band at 396 cm^{-1}, and bands at 253, 299, and 488 cm^{-1}, in addition to the magnetite band at 680 cm^{-1}. The Raman spectrum of goethite contains bands at 298, 396 and 480 cm^{-1}. A comparison of the Flake 2 spectrum with the goethite spectrum indicated that the broad band at 396 cm^{-1} in the flake could only partly be due to goethite; there are likely several overlapping bands, one from goethite, and the others due to unidentified components. This sample was partly covered in a yellow surface layer, consistent with the presence of goethite. This surface film may have been a result of oxidation during the handling and storage of the sample, and highlights one of the benefits of doing an in-situ inspection of the deposits.

The Raman spectrum labelled Flake 3, obtained from the third flake, contains a band due to magnetite at 684 cm^{-1}, and also bands at 490, 634, 1016 and 1087 cm^{-1}. The latter two bands are not shown in Figure 5. The band at 1016 cm^{-1} was quite intense in several of the spectra from the flake samples. This band may be due to a sulfate species; calcium sulfate has a strong Raman band at 1018 cm^{-1}.[12] The band at 1087 cm^{-1} may be due to a carbonate species.

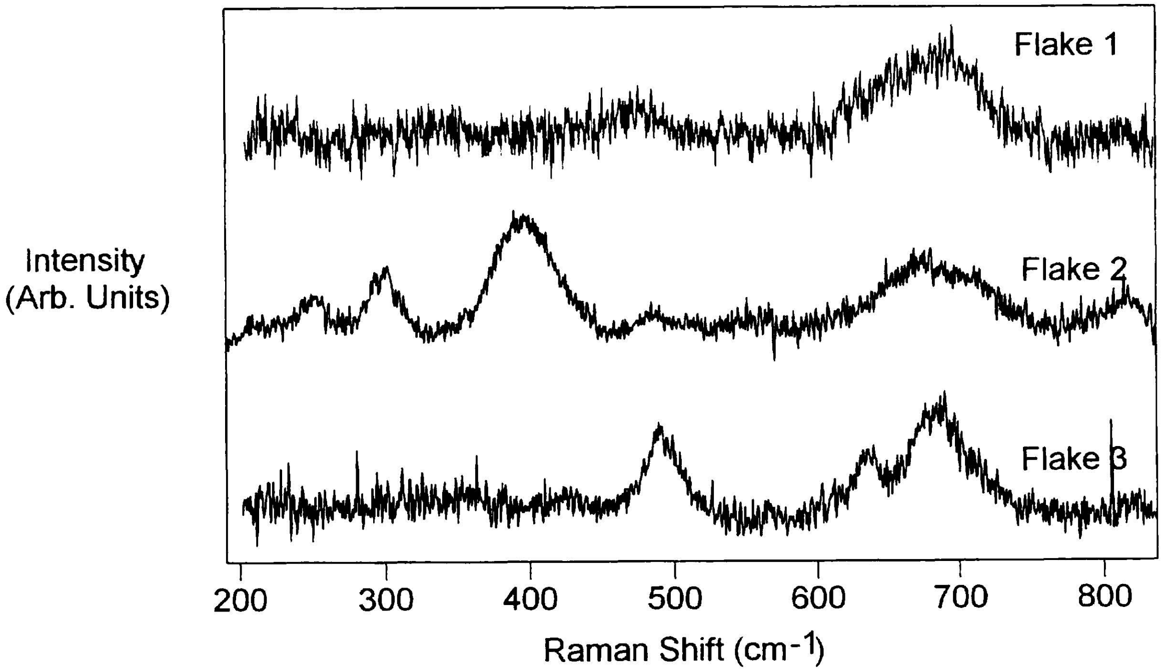

FIGURE 5: Raman spectra of three flake deposits

Figure 6 shows a spectrum of the secondary-side deposit on a piece of BNGS steam generator tube. Bands arising from hematite (marked with an H) and magnetite (marked with an M) are observed. Two weak bands of unknown origin, one a shoulder at 467 cm^{-1} and the other at 576 cm^{-1}, are also observed (marked by a U). The hematite detected may have been present in the original deposit; however, since the tube had been stored for over one year, the hematite may be a surface oxidation product of magnetite. A third possibility was the conversion of magnetite to hematite by the laser during the measurement. To minimise the latter process, the spectra were acquired using a laser power of roughly 3 mW incident at the sample. The acquisition time was 10 min.

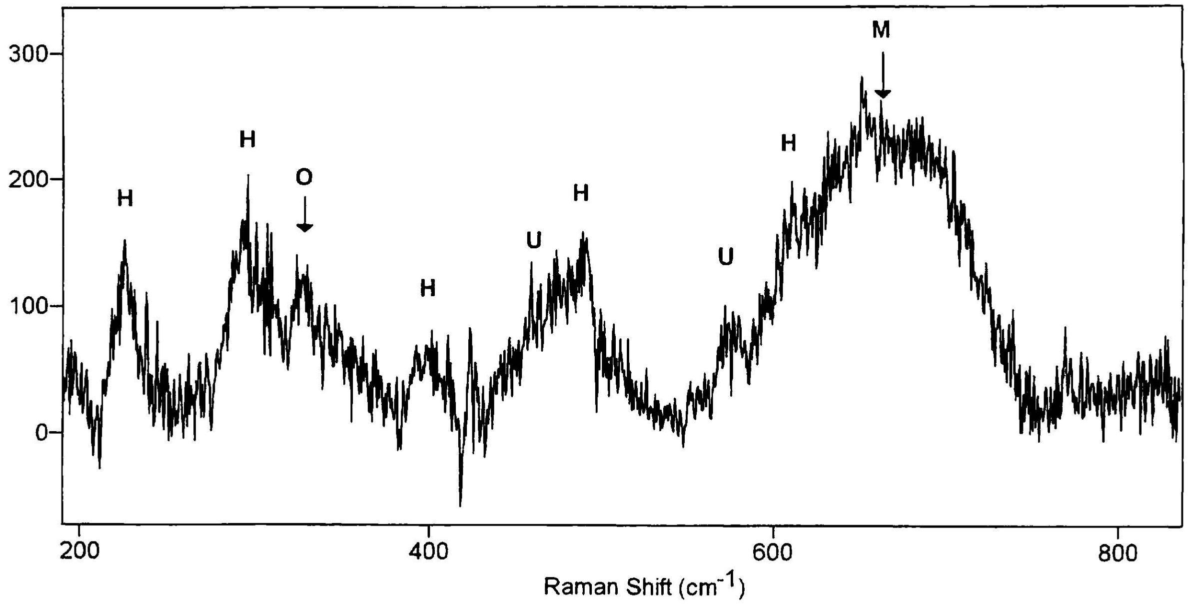

FIGURE 6: Raman spectrum from the secondary side deposit on a piece of BNGS SG tube. Labels denote bands due to magnetite (M), hematite (H), unknown components (U) and optical artefact (O).

Semi-quantitative Determination of Concentrations

The spectra from the PNGS deposit samples can be used to illustrate the ability of Raman spectroscopy to determine semi-quantitative compositions. Although the nickel ferrite and magnetite bands overlap in the 640-710 cm^{-1} spectral region, the peak height of the magnetite band, measured at 666 cm^{-1}, and the peak height of the nickel ferrite peak, measured at 700 cm^{-1}, were used to estimate the relative amounts of magnetite and nickel ferrite. For the two Pickering samples examined, the Raman spectra suggest that the ratio of nickel ferrite to magnetite is greater in the Unit 6 sample than in the Unit 5 sample.

In mixtures of particles of strongly absorbing oxides, such as magnetite, the intensities of the Raman bands do not vary linearly with the concentration of the oxide phases present. This is a result of a combination of light scattering and light absorption by the particles. However, quantification of the composition of such a mixture can be carried out using suitable calibration mixtures. Calibration mixtures of magnetite and hematite and of magnetite and nickel ferrite were prepared by mechanically mixing the pure powders to produce a homogeneous mixture. Calibration curves were measured for mixtures of magnetite and nickel ferrite, and of magnetite and hematite, prepared with different ratios of the two components. An empirical calibration curve was then fit to the data.

From calibration curves obtained from mixtures of magnetite and nickel ferrite, estimates of the relative amounts of magnetite and nickel ferrite were made. For the Unit 5 sample, 65 ±5% of the total spinel phase present was nickel ferrite and 35 ±5% was magnetite. The composition determined by other analytical techniques was 85% nickel ferrite and 15% magnetite, while Mossbauer spectroscopy suggested a composition of 47% nickel ferrite and 44% magnetite, with the remainder being zinc ferrite. The Raman results are therefore intermediate between these two analyses. For the sample from Unit 6, the Raman results suggest that the composition is richer in nickel ferrite; of the magnetite group spinels present, 75 ±5% was nickel ferrite and 25 ±5% was magnetite.

For these complex mixtures of closely related phases, the compositions determined by any of the analytical techniques used, while consistent with the analyses carried out, cannot be considered as "definitive" compositions. While the elemental compositions determined by NAA and ICP-AES are quite accurate, determination of the absolute amounts of the various, closely-related spinel phases (e.g., magnetite, nickel ferrite, zinc ferrite) in these mixtures is difficult by any technique. The similarity between the Raman results and those obtained by other analytical methods demonstrates the utility of Raman spectroscopy for semi-quantitative analysis of the major constituents of these deposits.

CONCLUSIONS

By careful optical filtering of the exciting laser line and the Raman-shifted light, good quality *ex-situ* Raman spectra of steam generator secondary-side deposits can readily be obtained using a fibre optic based Raman spectrometer. Spectra were obtained from powdered samples and millimetre-sized flakes, as well as from deposits on sections cut from pulled steam generator tubes. The major chemical phases, other than metallic copper, can be readily identified, and a semi-quantitative estimate of the composition can be made, as verified by comparison with deposit analyses performed using other techniques. This work demonstrates that *in-situ* characterisation of secondary-side deposits using fibre-optic Raman spectroscopy is feasible. A field trial of this technique should be carried out.

Laser-induced decomposition was noted for samples containing large amounts of magnetite. The decomposition usually resulted in the formation of hematite, and an increase in the intensity of hematite bands with time was a good indicator for decomposition. This decomposition was minimised by working at low laser powers and using a slightly defocused laser. The presence of water with the samples did not adversely affect the spectra, but rather improved the quality of the spectra obtained from the powder samples by minimising laser-induced decomposition.

The spectra obtained from the flake samples demonstrate the ability of Raman spectroscopy to detect local variations in the composition of these heterogeneous deposits. Several Raman bands were found that could not be definitively assigned to a particular chemical species; a larger database of Raman spectra of real and synthetic deposits is needed.

ACKNOWLEDGEMENTS

Funding for this work was provided by the CANDU Owners Group (COG), Technical Committee 19. The authors would like to thank COG for permission to publish this work. The authors would like to thank Bruce Nuclear Generating Station, Pickering Nuclear Generating Station, and Gentilly-2 Nuclear Generating Station for providing the samples studied in this work. The authors would also like to acknowledge J. Semmler for providing the XRD, ICP, and Mossbauer analytical data.

REFERENCES

1. T.F. Habib, P.A. Sherburne, J.F. Dunne and C.L. Williams, "Degradation in Ginna Steam Generator Tube Heat Transfer due to Secondary-side Fouling", Steam Generator Sludge Deposition in Recirculating and Once Through Steam Generator Upper Bundle and Support Plates, NE-Vol. 8, ASME, (1992).

2. C.W. Turner and S.J. Klimas, "Thermal Resistance of Boiler Tube Deposits at Steam Generator Operating Conditions", Proceedings: Sludge Management Workshop, EPRI Report TR-104212 (1994).

3. R. Dyck, P. Spekkens, K. Verma and A. Marchand, "Operational Experience with Steam Generators in Canadian Nuclear Plants", Proceedings of the Steam Generator and Heat Exchangers Conference, Vol I, Canadian Nuclear Society, Toronto, Canada (1990).

4. L.E. Johnson, "Fouling in Nuclear Once-Through Steam Generators", WA/NE-12 ASME Winter Annual Meeting, Paper 87 (1987).

5. W.A. Byers, P.J. Kuchirka, M. Rootham and A.J. Baum, "Can Traces from the Past Predict the Future?", Electric Power Research Institute Surface Chemistry Workshop (1996).

6. C.W. Turner and K. Shamsuzzaman, "The Role of Copper in Sludge Consolidation", Proceedings: Sludge Management Workshop, EPRI Report TR-104212 (1994).

7. I.R. Lewis and P.R. Griffiths, "Raman Spectroscopy with Fibre Optic Coupling", Appl. Spectrosc. 50, 12A (1996).

8. J. Andrews, "Raman Spectroscopy Moves On-Line", Spectroscopy Europe, 7, 8 (1995).

9. J. Gui and T.M. Devine, "In-situ Vibrational Spectra of the Passive Film on Iron in Buffered Borate Solution", Corrosion Science, 32, 1105 (1991).

10. J. Dunwald, and A. Otto, "An Investigation of Phase Transitions in Rust Layers Using Raman Spectroscopy", Corrosion Science, 29, 1167 (1989).

11. R.J. Thibeau, C.W. Brown and R.H. Heidersbach, "Raman Spectra of Possible Corrosion Products of Iron", Appl. Spectrosc., 32 , 532 (1978).

12 S.D. Ross, Inorganic Infrared and Raman Spectra (London, UK: McGraw Hill, 1972)

13. K.F. McCarty, D.R. Boehme, "A Raman Study of the Systems $Fe_{3-x}Cr_xO_4$ and $Fe_{2-x}Cr_xO_3$", J. Solid State Chem., 79, 19 (1989).